GALVANOSTATIC DEPOSITION OF HIERARCHICAL LAYERED α-MoO₃ THIN FILMS AND ITS CHARACTERIZATION TO STUDY THE INFLUENCE OF HEAT TREATMENT

A. SASI[*], C. SASIKUMAR

Department of Material Sciences & Metallurgical Engineering, MANIT, Bhopal-462003, M.P, India

Orthorhombic molybdenum oxide (α-MoO3), thin films have been grown on stainless steel (SS-304) substrates from acidic ammonium heptamolybdate $[(NH_4)_6Mo_7O_{24}.4H_2O]$ aqueous solution by Potentiostat-Galvanostat electrolysis process. The crystal structure and surface morphology of the as-grown films have been investigated by X-ray powder diffraction (XRD), Fourier Transform Infrared Spectra (FTIR), and Field Emission Scanning Electron Microscopy (FESEM). The results of XRD and FTIR analyses have confirmed the formation of layered orthorhombic structure. Particle size is found to increase from 32 nm to 40 nm with thermal oxidation. The FESEM results clearly depicted the morphology of α-MoO₃. The morphology study showed the final product comprises of plate – shaped particles stacked in layered form.

1. Introduction

Transition metal oxide due to their unusual and enhanced properties has attracted considerable attention. Among all transition metal oxides, the characterization of molybdenum trioxide which prepared by different techniques in various nanostructure morphologies has proven great potential in many applications such as photochromic and electrochromic devices, catalysts, gas sensors, photovoltaic cells, batteries and many more [1-5]. There are two most common polymorphisms of MoO_3, first the orthorhombic MoO_3 (α-MoO_3), which is a thermodynamically stable phase and the metastable monoclinic MoO_3 (β-MoO_3), with a ReO_3-type structure respectively [6-9]. The α-MoO_3 is of particular interest as it has layered structured. The thickness of layers is 0.7 nm and exist in double layers of link where highly asymmetrical MoO_6 octahedral are interconnected with their edges along [001] direction and interlinked with their corners along [100] [10-14]. Atoms within the double layers are dominated by strong covalent and ionic bonding while the layers along [010] plane are linked only through weak van der Waal's forces. It has been shown that the reduction in the number of layers gives an increment in the carrier mobility of the material [12]. The β-MoO_3 structure doesn't have MoO_6 octahedral along the [001] plane nor forms the double layers like α-MoO_3 [14, 15]. There are abundant synthetic techniques reported for the development of MoO_3, such as chemical vapor deposition, pulse laser deposition, thermal evaporation, sol-gel, sputtering, hydrothermal, anodization and electrodeposition [16-24].

In the middle of all, electrochemical methods are profitable, as they are easy to perform and offer too simple control over morphology, thickness, extend to oxidation and doping at room temperature which makes the process versatile and compatible with electronic device industry standards [25].

In the present communication, the layered orthorhombic MoO_3 (α-MoO_3) were effectively prepared by electrodeposition from heptamolybdate aqueous solutions. This study provides a simple and novel route for the preparation of orthorhombic MoO_3. In particular, the influence of thermal oxidation on its structural and morphological properties of MoO_3 films were studied which will be useful for practical application in the future.

*Corresponding author: arshalishashi83@gmail.com

2. Experimental

2.1 Electrodeposition of Molybdenum oxide thin films

All the chemical reagents used in this work were analytical grade and are used without further purification. Molybdenum oxide thin films were prepared in an electrolytic cell using a potentiostat (Gamry, model reference 600) with three electrode system.
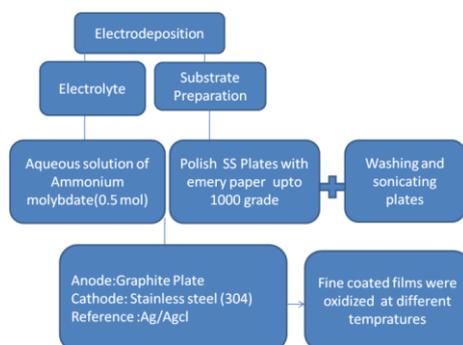

Fig. 1. Schematic representation of synthetic procedures for the molybdenum trioxide thin films by electrodeposition method

The bath solution of 0.05 M was prepared by dissolving essential amount of ammonium heptamolybdate $[(NH_4)_6Mo_7O_{24}.4H_2O]$ to 500 ml of triple distilled water. The pH value of the mixture was adjusted to 2 with the addition of Sulfuric acid. The electrodeposition was conducted at a cathodic current density of 2 mA/cm^2 for different times. A high purity graphite plate was used as a counter electrode, Ag/AgCl used as a reference electrode and stainless steel sheet as working electrode. For each test, a newly prepared solution was employed. After each coating, the films were washed with ethanol and dried in air. Finally, the fine coated films were given temperature in the presence of oxygen in a standard horizontal furnace with heating and cooling ramp rate of 1°C/min.

2.2 Characterization of MoO_3 samples:

The as-synthesized and annealed thin films were characterized for their optical and nanostructure properties. The phase and crystallinity of the films was investigated by using Philips - X-ray diffractometer operating at 40 KV-30 mA using CuK$_\alpha$ radiation of wavelength λ= 0.541 nm in the scan range $2\theta = 10°$ to 80°. Morphology of the samples was investigated using a field emission scanning electron microscope (FESEM) and Energy Dispersive X-ray Analysis (EDAX) has been used for compositional analysis of the molybdenum films. IR experiments were performed on the samples on a Fourier transform infrared (FTIR) spectrometer.

3.Results and discussion

3.1 XRD Analysis

The XRD pattern recorded on an X-Ray diffractometer for the as-synthesized and thermal oxidized thin films confirmed the crystallinity, structure and phase purity. Figure 2 (a-d) shows the XRD pattern of the as- synthesized and annealed samples at 350°C,450°C and 550°C respectively. The depth analysis of XRD patterns have showed that MoO_3 films have crystallized in α-MoO_3 orthorhombic structure as on increasing the temperature. The distinct peaks which match up to MoO_3 indicate the crystalline quality of the films. The observed lattice constants ($a = 3.9620 \, \mathring{A}$, $b = 13.8550 \, \mathring{A}$, $c = 3.7010 \, \mathring{A}$) are in good agreement with the reported values (JCPDS card no: 089-5108). Moreover, the sharpness of the peaks increases gradually with an increase in the thermal oxidation. Diffraction peaks due to the intermediate phases such as MoO_2, Mo_4O_{11}, and

Mo_9O_{26} were also found to appear in the diffraction patterns. In fact, this phase dominate the MoO_3 in terms of intensity in beginning and gradually disappears with thermal oxidation.

The Scherrer's method is used to calculate the crystallite size D_{hkl} with the assumption of negligible strain [26],

$$D_{hkl} = k\lambda \frac{\beta_{size}}{cos\theta_{hkl}} \qquad (1)$$

Where k the shape factor (0.9) is, θ_{hkl} is the Bragg diffraction angle and λ is the wavelength of Cu Kα_1 radiation (1.5406 Å). The crystallite size was increasing from 34 to 40 nm with an increase of oxidation temperature.

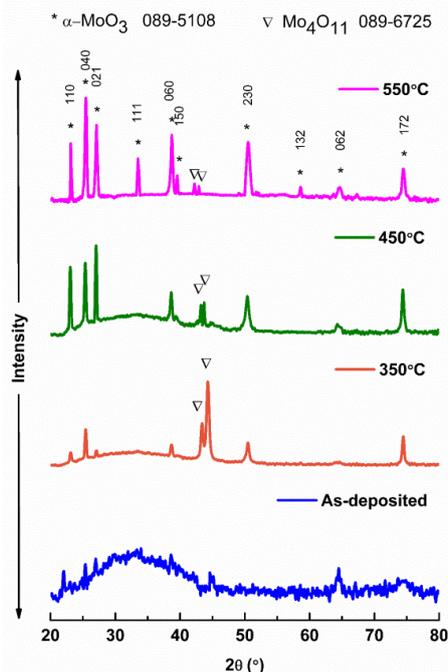*Fig. 2: XRD pattern of MoO₃ films electrodeposited at pH 2 and at different temperatures (a) as-deposited, (b) 350°C, (c) 450°C, and (d) 550°C*

3.2 Morphological and Elemental analysis

The FESEM micrograph images of the as-deposited and the molybdenum oxide films at different heating temperatures are shown in Figure 2 (a-d). Image of as-deposited films showed even surface morphology Figure 2 (a). The films at 350°C in figure 2 (b) shows as the molecules started acquiring the required thermal energy to promote the growth of polycrystalline MoO_3 with the larger grain size. As on increasing the heating temperature at 450°C with pH 2 in Figure 2 (c) shows the formation of platelet nanocrystallites distributed uniformly over the surface with the grain size of about 600 nm, due to the coalescence of nearby crystallites which were driven by the thermal energy gained during heating. At 550°C shown in Figure 2 (d) these platelets started to join together to form a layered structure which gives an indication of the formation of the α-phase MoO_3 [13, 27]. Additionally, from EDAX analysis it is seen that only Molybdenum and Oxygen are present in the sample (550°C), no other impurities are present. Thus, the morphological studies confirmed that the thermal oxidation of films does the modification in grain area which leads to the enhancement in crystalline structure of α-phase MoO_3. Figure 4 shows the EDAX spectrum of the MoO_3 film annealed at 550°C. The elemental composition of the films shows characteristic constituents of molybdenum and oxygen are present. This indicates that the formation of desired compound.
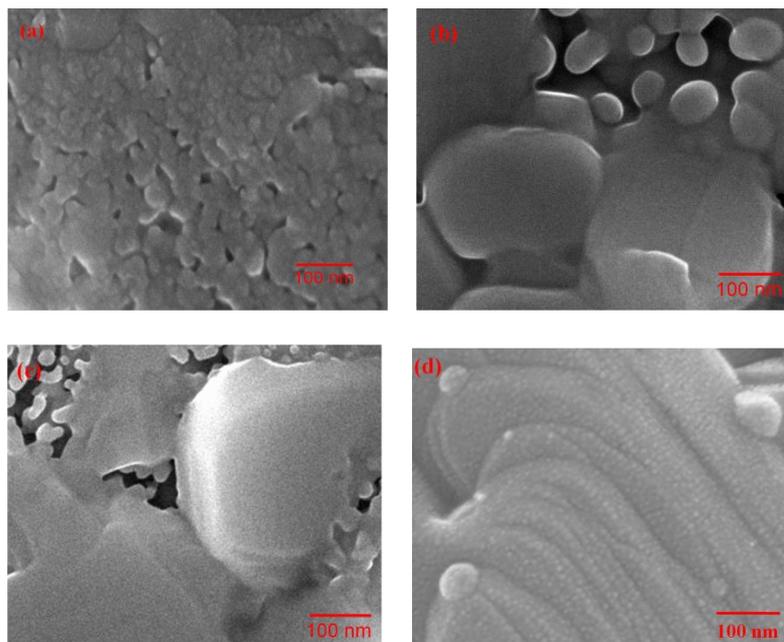
Fig. 3: Electron micrographs of MoO₃ films electrodeposited at pH 2 and at different temperatures (a) as-deposited, (b) 350°C, (c) 450°C, and (d) 550°C
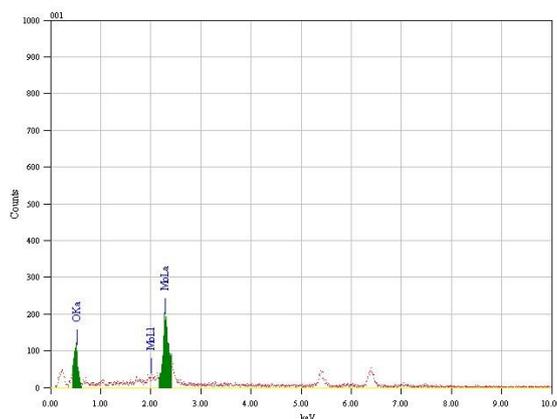

Fig. 4: EDAX pattern of MoO₃ films electrodeposited at pH 2 and at 550°C.

3.3 Functional Group Analysis

The functional groups present in the synthesized films were analyzed using FTIR spectrophotometer (Perkin Elmer) at the resolution of 4 cm^{-1} in the range of 4000 - 400 cm^{-1} shown in figure 5. IR spectra analysis also confirms the formation of layered α-MoO$_3$ phase in the hierarchical structure as on increasing the heating temperature. It can be seen that there are absorption peaks at 550 cm^{-1}, 889 cm^{-1}, 990 cm^{-1}, 1610 cm^{-1} and 3400 cm^{-1}, which is shown in the shaded portion of the spectrum. According to the study conducted by Zakharova et al. [28], the thermally treated samples had strong vibrations that were detected as mentioned above, respectively. The confirmation of the layered orthorhombic MoO$_3$ phase in IR spectrum is assign to the stretching mode of oxygen in the Mo-O-Mo units and the Mo=O stretching mode at 990 cm^{-1} [28, 29]. Absorption band at 3400 cm^{-1} and 1610 cm^{-1} were also observed in the spectrum which is due to the hydrogen-bonded water molecules. These absorption peaks starts vanishing with the heating temperature as the water group coordinated with Mo atoms starts removing from the films.
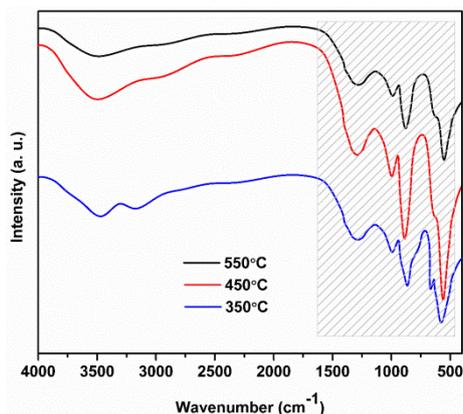
Fig. 5: FTIR of MoO₃ films electrodeposited at pH 2 and at different temperatures
(a) as-deposited, (b) 350°C, (c) 450°C, and (d) 550°C

4. Conclusion

We demonstrated the simpler and easier processes for producing α-MoO_3 thin films on SS-304 substrates by an electrochemical method with different oxidation temperatures. The crystallite size was about 30-40 nm, and the particles formed plate shaped structure stacked into layered form when heated at 550°C. When the samples were heated at temperatures ranging from 200 to 550°C, there was an increase in intensity of intermediated phase such as Mo_4O_{11} which gradually disappeared at 550°C. The results of XRD analysis and FTIR have confirmed the formation of layered α-MoO_3 with orthorhombic crystal system at 550°C thermal oxidation. The cell parameters of the unit cell are determined as ($a = 3.9620\ \mathring{A}$, $b = 13.8550\ \mathring{A}$, $c = 3.7010\ \mathring{A}$) respectively. The FESEM micro structural study discovered a good homogeneity across the entire surface of each film.

References

[1] P. Carcia, E. McCarron, Thin Solid Films **155**(1), 53 (1987).
[2] X. W. Lou, H. C. Zeng, Chemistry of materials **14**(11), 4781 (2002).
[3] N. A.,Chernova, et al., Journal of Materials Chemistry **19**(17), 2526 (2009).
[4] T. Mizushima, et al., Applied Catalysis A: General **326**(1), 106 (2007).
[5] L. Boudaoud, et al., Catalysis today **113**(3), 230 (2006).
[6] W.-C. Chang, et al., CrystEngComm **13**(16), 5125 (2011).
[7] S.-Y. Lin, et al., Journal of sol-gel science and technology **53**(1), 51 (2010).
[8] J. S. Chen, et al., The Journal of Physical Chemistry C **114**(18), 8675 (2010).
[9] L. Zhou, et al., The Journal of Physical Chemistry C **114**(49), 21868 (2010).
[10] V. Bhosle, A. Tiwari, J. Narayan, Journal of applied physics **97**(8), 083539 (2005).
[11] S.Sunu, et al., Sensors and Actuators B: Chemical **94**(2), 189 (2003).
[12] K. Kalantar-zadeh, et al., Chemistry of Materials **22**(19), 5660 (2010).
[13] I. Navas, et al., Journal of Physics D: Applied Physics **42**(17), 175305 (2009).
[14] M. Gacitua, et al., physica status solidi (a) **207**(8), 1905 (2010).
[15] C. Ramana, C. Julien, Chemical physics letters **428**(1), 114 (2006).
[16] B. Wang, et al., Journal of Alloys and Compounds **661,** 66 (2016).
[17] C. Ramana, et al., Journal of Vacuum Science & Technology A: Vacuum, Surfaces, and Films **25**(4), 1166 (2007).
[18] Y. Xie, et al., The Journal of Physical Chemistry C **114**(1), 120 (2009).
[19] D. Parviz, et al., Journal of Nanoparticle Research, **12**(4), 1509 (2010).
[20] S. Dayal, C. S. Kumar, Materials Research Express, **3**(10), 106405. (2016).
[21] K. Dewangan, et al., CrystEngComm **13**(3), 927 (2011).

620

[22] T.M. McEvoy, et al., Langmuir **19**(10), 4316 (2003).

[23] B. M. Sanchez, et al. *An Investigation of Nanostructured Thin Film α-MoO₃ Based Supercapacitor Electrodes in an Aqueous Electrolyte*. in *Meeting Abstracts*. 2012. The Electrochemical Society.

[24] D. D. Yao, et al., Crystal Growth & Design,**12**(4), 1865 (2012).

[25] V. Nirupama, et al., Current Applied Physics **10**(1), 272 (2010).

[26] P. Jain, S. Srivastava, Journal of Superconductivity and Novel Magnetism **29**(8), 2089 (2016).

[27] W.-Q. Yang, et al., Physics Letters A **373**(43), 3965 (2009).

[28] G. Zakharova, et al., Solid State Sciences **9**(11), 1028 (2007).

[29] M. Dhanasankar, K. Purushothaman, G. Muralidharan, Applied Surface Science **257**(6), 2074 (2011).